



## MEASUREMENT OF RADIOACTIVE AEROSOLS AS AN ORIGINAL INDICATOR OF ATMOSPHERIC POLLUTION IN URBAN AREAS

G. Le Petit\*, J.-C. Milliès-Lacroix\* and F. Simon\*\*

\*Commissariat à l'Energie Atomique, Direction des Recherches en Ile-de-France  
Département Analyse et Surveillance de l'Environnement, Service Radioanalyses  
Chimie et Environnement, BP 208 91311 Montlhéry Cedex, France

\*\*AIRPARIF Surveillance de la Qualité de l'air en Ile-de-France,  
10, rue Crillon Paris Cedex 04, France

### ABSTRACT

*The Service Radioanalyses, Chimie et Environnement (Département Analyses Surveillance de l'Environnement) of the French Atomic Energy Commission, located in suburban Paris, has for many years been conducting atmospheric radioactivity measurements. Since 1994, the laboratory has been using high volume air samplers equipped with filters for the weekly collection of atmospheric aerosols at a mean rate of about  $600 \text{ m}^3 \cdot \text{h}^{-1}$ . The polypropylene filters, with a collection efficiency in excess of 93%, are compacted after sampling. The atmospheric radioactivity is measured by HP Ge gamma spectrometry after decay of short-lived natural relationship products.*

*A study conducted in 1996 shows good correlation between the evolution with time of some of the indicators routinely used by AIRPARIF, the organization in charge of monitoring the air quality in the Ile-de-France region, to measure atmospheric pollution in the Paris area ( $\text{SO}_2$ , NO) and that related to radioactivity of terrestrial ( $^{210}\text{Pb}$ ,  $^{40}\text{K}$ ) and anthropogenic ( $^{137}\text{Cs}$ ) origin, as well as the amount of aerosols collected. Further, the distribution in time of the atmospheric radioactivity of cosmogenic origin ( $^7\text{Be}$ ) shows a yearly evolution somewhat similar to that observed with ozone.*

### INTRODUCTION

The Montlhéry laboratory of the Service Radioanalyses, Chimie et Environnement (SRCE) has been making atmospheric radioactivity measurements since the sixties, and participates in international intercomparisons involving the entire high-volume aerosol sampling and radiometric analysis. Daily radiological monitoring of the environment over a large number of years allows short term and long term evolution of the atmospheric radioactivity to be emphasized. Further, knowledge of the local radiological concentrations makes it possible to detect a possible nuclear industry contribution at an early stage.

The use of high-volume (over  $500 \text{ m}^3 \cdot \text{h}^{-1}$ ) aerosol samplers and the level of performance achieved over the last few years by HP Ge gamma spectrometry allows minimum concentrations of about one microbecquerel per  $\text{m}^3$  to be detected for a filtered air volume of about  $100\,000 \text{ m}^3$ . Under these conditions, determining the specific activity

of the main atmospheric radionuclides, with an uncertainty generally less than 30%, allows seasonal fluctuations to be emphasized. The observation of an analogy with the evolution in time of the major atmospheric pollutants measured in the Paris area could be valuable for helping to understand the mechanisms which govern the overall evolution of atmospheric radioactivity.

## SAMPLER AND FILTERING MEDIA USED

### ASS500 P sampler

The high-volume aerosol sampler used is the ASS500 P type (Fig. 1). This unit is manufactured by Germany's Physik Technik Innovation (PTI) of Erlangen (Arnold *et al.*, 1994). About twenty units are currently installed, in western Europe and eastern Europe (Belarus, France, Germany, Iceland, Poland, Spain, Sweden, Switzerland). The Montlhéry laboratory (2° 14' E, 48° 37' N), 30 km to the South South-West of Paris in France also operates an ASS500 P sampling station in French Polynesia, as part of a southern hemisphere atmospheric monitoring programme.

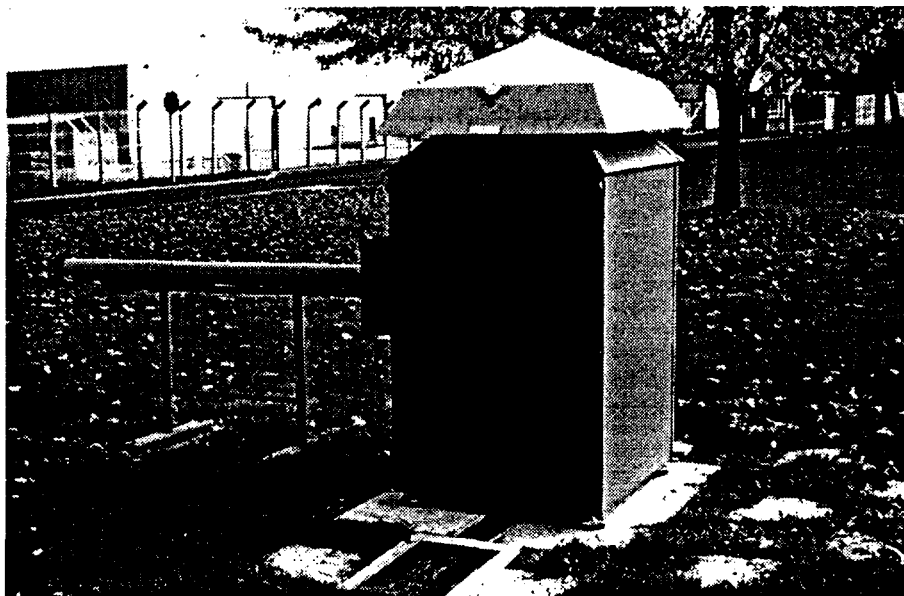


Fig. 1. ASS500 P sampler

The ASS500 P sampler is used on a continuous basis under severe weather conditions. The horizontal sampling head is protected by an aluminum cover (Fig. 2). The filter, with 44 x 44 cm useful dimensions, is installed on a calibrated grid support and sealed. Two infrared tubes are installed above the filter to prevent frost in winter time. The ASS500 P is equipped with a device indicating the filtered air volume at a given time and the instantaneous air flow. The mean air flow for a 24-hour sampling period is about  $750 \text{ m}^3 \cdot \text{h}^{-1}$ , and  $600 \text{ m}^3 \cdot \text{h}^{-1}$  for weekly samplings. The filtered air volumes over a one-week period are about  $100\,000 \text{ m}^3$ . The air flow depends on the type of filter used to collect the atmospheric aerosols. Fig. 3 shows a typical profile of the filtered air flow variation over a one-week sampling period using a polypropylene filter (type G3, marketed by PTI), with a surface density of about  $125 \text{ g} \cdot \text{m}^{-2}$ .

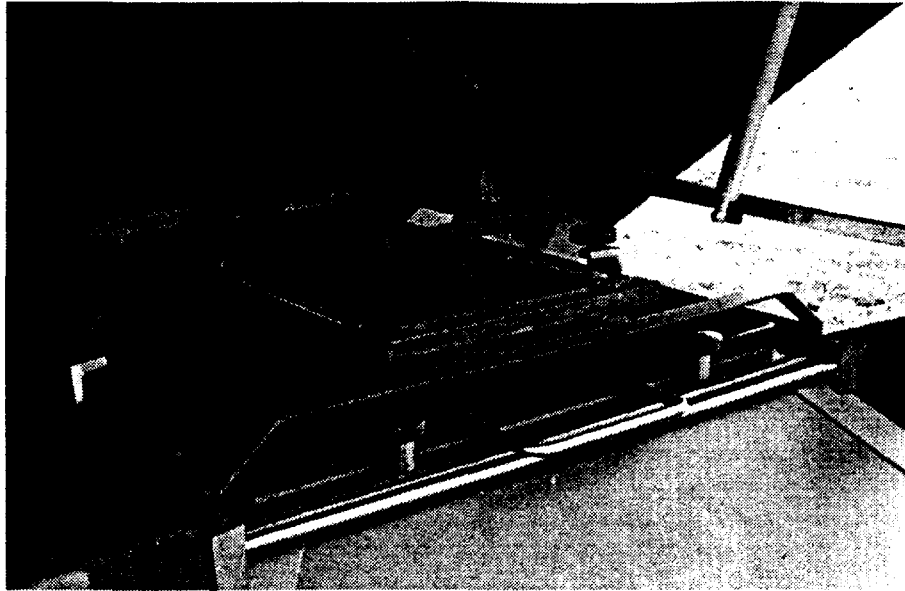


Fig. 2. Sampling head with filter mounted horizontally

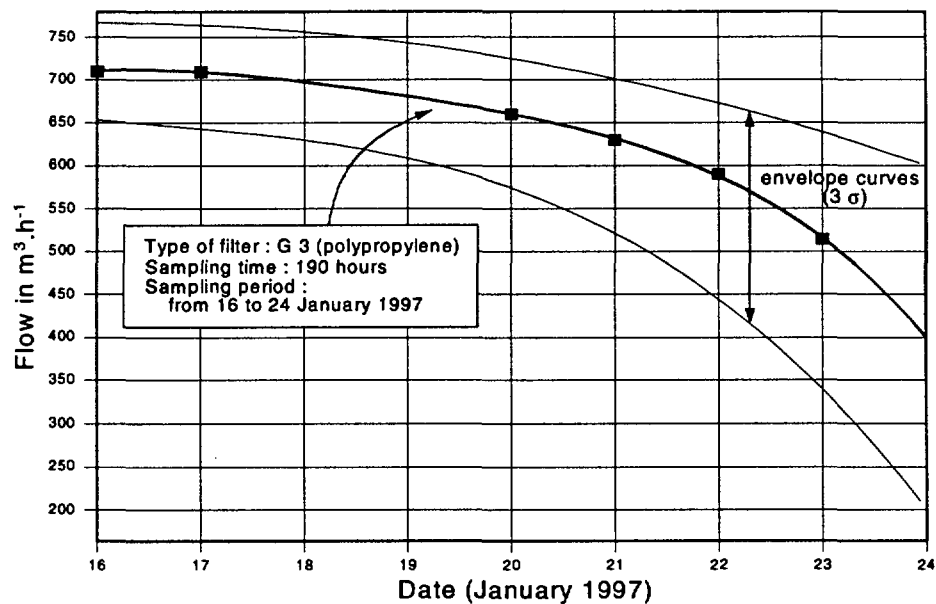


Fig. 3. Flow variation of the ASS500 P over a one-week sampling period.

Further, the mean weekly flow, and by correlation, the filtered air volume, varies significantly as a function of the weather conditions observed during the sampling period. At certain times of the year, the atmospheric dust level may lead to a significant drop in the flow and to filter clogging. Fig. 4 shows the mean weekly flows obtained during 1996. We can see that they are generally lower at the beginning of the year (with a minimum in January, i.e.  $420 \text{ m}^3 \cdot \text{h}^{-1}$  corresponding to a weekly volume of  $69\,190 \text{ m}^3$ ) than at the end of the year (with a maximum in November, i.e.  $730 \text{ m}^3 \cdot \text{h}^{-1}$ , corresponding to a volume of  $140\,000 \text{ m}^3$ ). The minimum mean flow reached in 1996 for a one-week sampling is  $370 \text{ m}^3 \cdot \text{h}^{-1}$ .

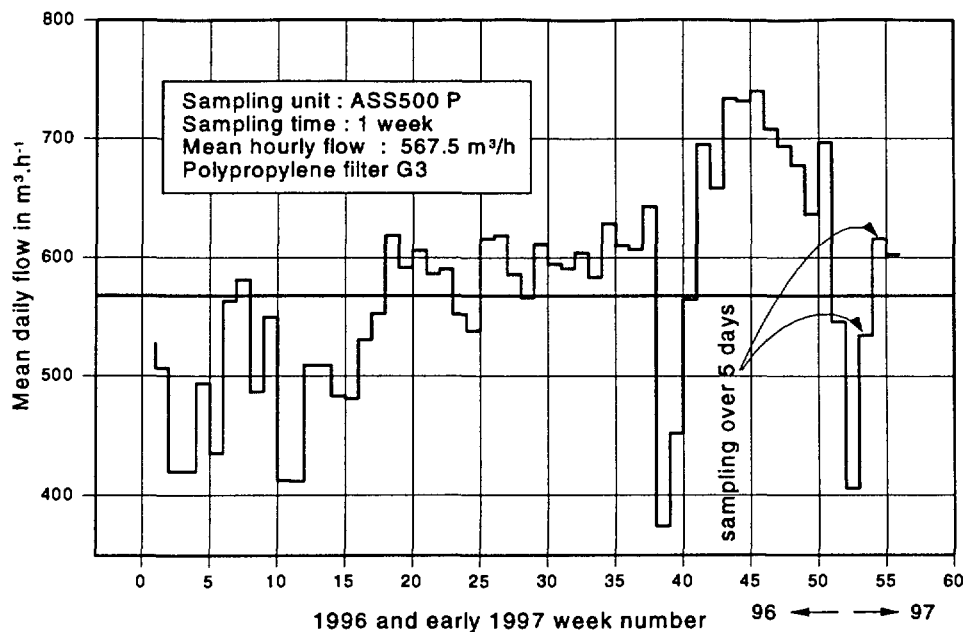


Fig. 4. Yealy variation of the ASS500 P weekly flow

### Filtering media

The aerosols consist of a mixture of polydisperse size particles. The particle-size range of the atmospheric aerosols in non-urban areas, varies as emphasized by several writers (Karol L., 1964; Pruppacher H.R. *et al.*, 1983), ranges from 0.01 to about 20  $\mu\text{m}$ . Further, the size distribution of the particles varies as a function of the weather conditions during the sampling period (Fig. 5). The filtering medium used for sampling should therefore exhibit high efficiency over the complete particle-size range of the collected aerosols.

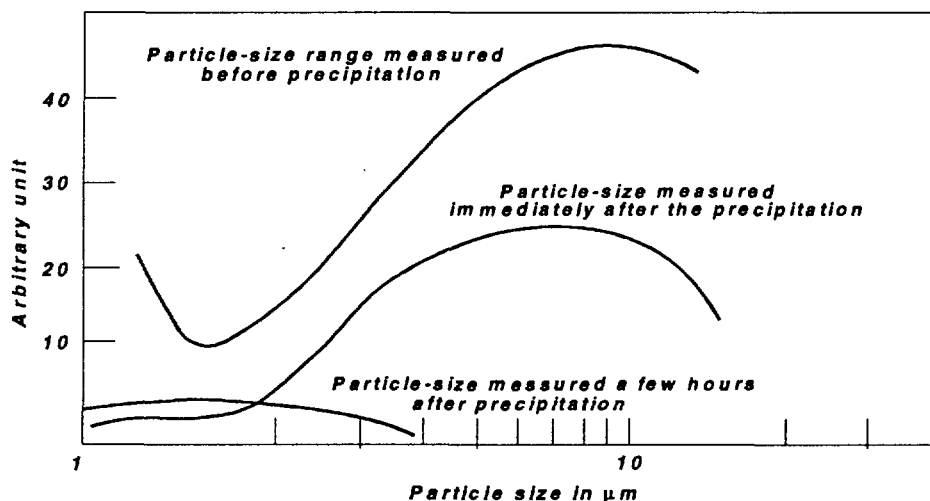


Fig. 5. Example of variation of the particle-size range of the aerosols under the effect of changing climatic conditions (cold front moving forward in the above case)

Many theoretical studies, in particular Davies (1973), indicate that for a given filter, the aerosol trapping efficiency is minimum for particles with a diameter of about 0.1  $\mu\text{m}$ . Further, the capture mode is highly dependent on the diameter of the particles and their velocity. There

are three main mechanisms for trapping aerosols on a filtering medium made of fibers, i.e.: capture by Brownian diffusion of the particles, capture by inertia and capture by interception (Fig. 6).

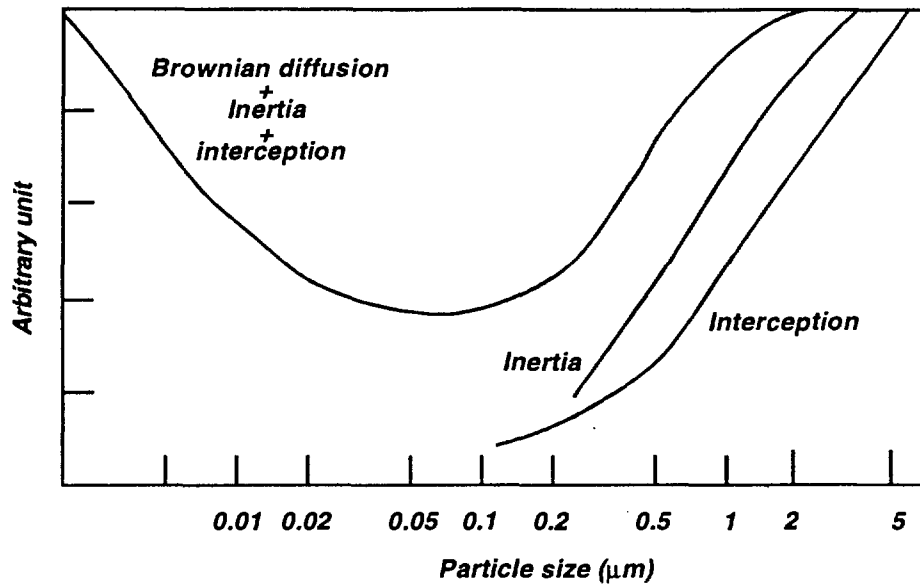


Fig. 6. Presentation of the various aerosol capture mechanisms as a function of particle size (Davies, 1973)

The ASS500 P sampler, equipped with a G3-type polypropylene filter operates at a filtration velocity of about  $2 \text{ m.s}^{-1}$ , which results in aerosol capture essentially by inertia and interception-diffusion (Fig. 7).

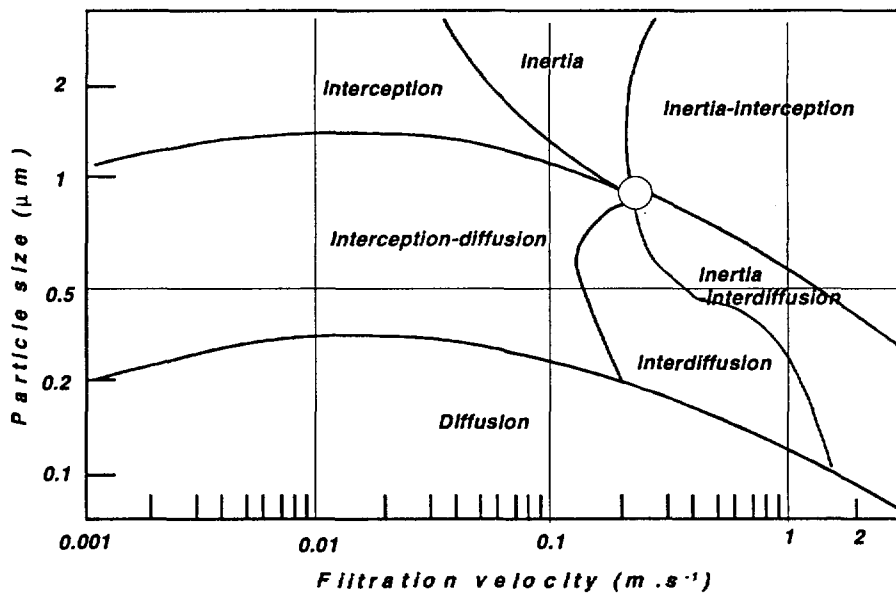


Fig. 7. Presentation of the various aerosol capture mechanisms as a function of particle size and filtration velocity (Davies, 1973)

The filtering medium was selected with regard to a number of parameters, i.e. capture efficiency, filter resistance during sampling, achieved filtration flow, reproducibility of the filter screen and feasibility of radiochemical analysis after sampling. Three types of filters has

been tested, i.e. two polypropylene filters weighting  $125 \text{ g.m}^{-2}$  (G3 type) and  $220 \text{ g.m}^{-2}$  (P414 type) respectively, and one chlorinated polyvinyl filter (type Petrianov FPP 15-1.5) weighting  $78 \text{ g.m}^{-2}$ . The collection efficiency and the underpressure characteristics of the various filters (at filtration velocities between  $0.25$  and  $2.5 \text{ m.s}^{-1}$ , were determined by the French Institut de Protection et de Sûreté Nucléaire (Sanchez *et al.*, 1995). The aerosol used, implemented in accordance with French standard NF X 44-011, is soda fluorescein with a  $0.15 \mu\text{m}$  median diameter and a particle-size distribution standard deviation of 1.6. The aerosol collection efficiency, characterized by the amount of aerosol captured by the filter, is shown in Fig. 8 for each type of filter.

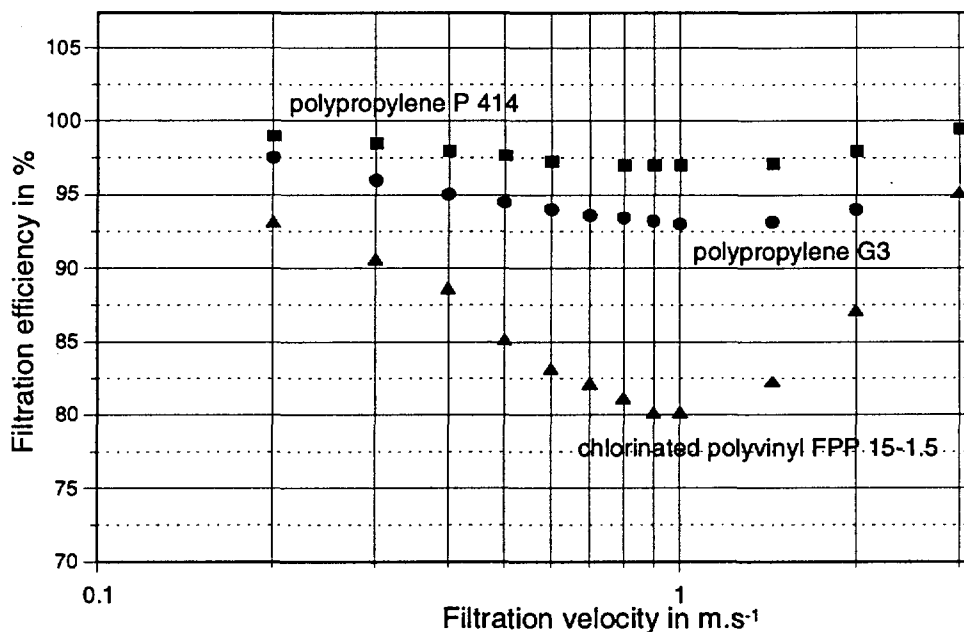


Fig. 8. Filtration efficiency of filters G3, P414 and FPP15 I-5

We can see that a minimum is obtained for all three filters near a filtration velocity of  $1 \text{ m.s}^{-1}$ . The polypropylene filter (P414 type) exhibits the best collection efficiency (about 97.5% at  $1 \text{ m.s}^{-1}$ ) against 93% (polypropylene G3 type) and 80% for the chlorinated polyvinyl filter (FPP15-1.5 type), respectively. Fig. 9 shows the underpressure obtained for the three filters. We can see that it varies linearly as a function of the filtration velocity, and as stated by the theory, the most efficient filter is that which exhibits the highest underpressure.

Although the efficiency of filter P 414 is higher, we selected for the ASS500 P samplers the polypropylene filter of G3 type, manufactured in Poland (distributed by PTI). This filter offers the advantage of a good collection efficiency because of a lesser underpressure, while offering more reproducible thickness characteristics. Fig. 10 shows the yearly distribution of the filter weight before installation on the sampler. We can note some degree of heterogeneity due to variations in the filter thickness. This can result in an increase of the filter weight of up to 15% more than the mean yearly value, slightly affecting the filter underpressure. The G3 filter further offers the advantage over filter P 414 of easier hot compaction for a defined geometry measurement of aerosols by HP Ge spectrometry.

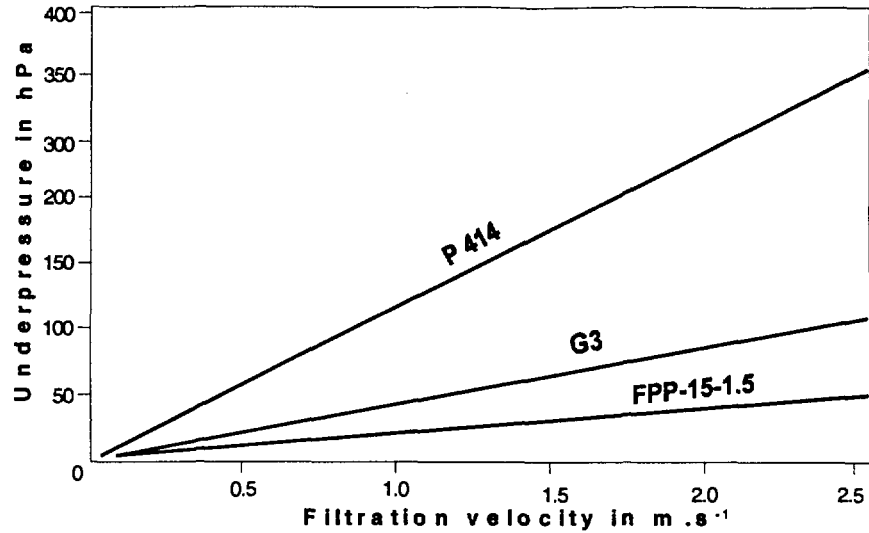


Fig. 9. Underpressure of filters G3, P414 and FPP 15 1-5

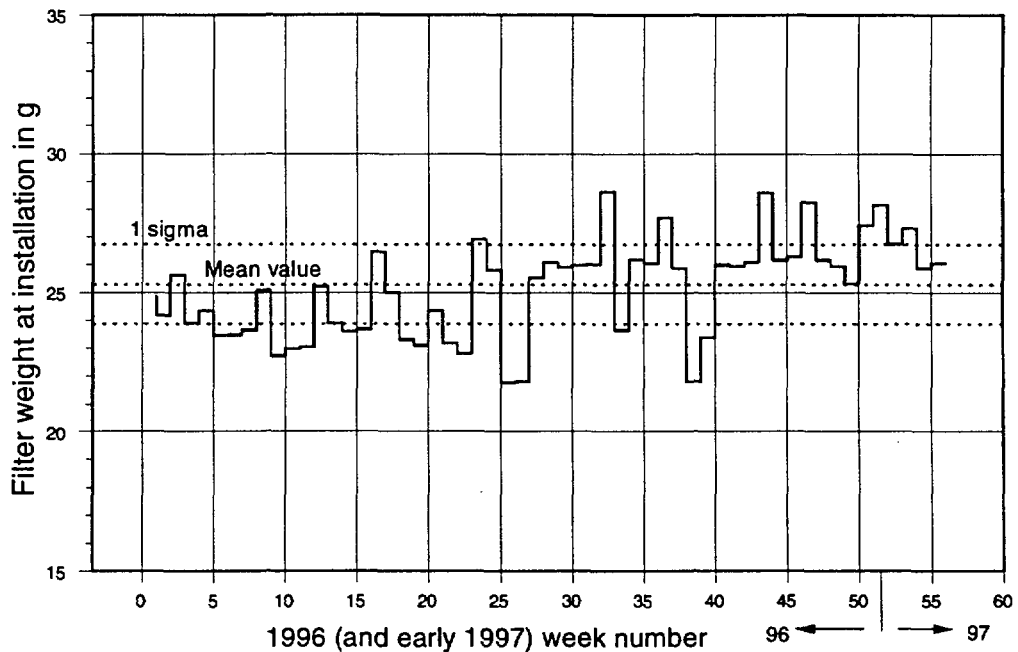


Fig. 10. Yearly variation of the weight of type G3 blank filters before installation on the ASS500 P

### Comparison of ASS500 P and CASA 110 sampler efficiency

The SRCE has routinely been taking atmospheric samplings using samplers other than the ASS500 P (CASA 110 manufactured by EUROVERRE, modified by BERTIN), for many years. A paper presented in Warsaw (Milliès-Lacroix *et al.*, 1994) describes the characteristics of this sampler which operates at a lower flowrate ( $100 \text{ m}^3 \cdot \text{h}^{-1}$ ) and presents the specific activities of the atmospheric radionuclides measured at Montlhéry and in French Polynesia. A comparison conducted over a highly significant number of measurements (two years of samplings) clearly indicates that the ratio of specific activities measured concurrently on both

samplers differ, even allowing for the uncertainty assigned to sampling and measurement. As an example, we have obtained a mean ratio of about 0.77 (ASS500 P/CASA 110) for  $^7\text{Be}$  and 0.84 for  $^{210}\text{Pb}$ . In order to explain this phenomenon we will investigate the dependence of the particle size at the filter head. This explanation is backed by the fact that the ratios (ASS500 P/CASA 110) for  $^7\text{Be}$  and  $^{210}\text{Pb}$  are different for measurements made in French Polynesia (about 0.60 for both radionuclides). This phenomenon will be discussed in a paper soon to be released.

### SAMPLING AND MEASUREMENT PROTOCOL

Atmospheric aerosol sampling is carried out for one-week periods. Each filter which equips the sampler is placed in an oven for 6 hours at  $90^\circ\text{C}$  then weighed on a precision scale, before installation on the ASS500 P. After removal, the filter is again dried and weighed. In general the weight loss after drying is about 1 gram, i.e. about 4% of the total weight. The filter is then hot-compacted ( $100^\circ\text{C}$  for 6 minutes) using a  $100\text{ kg.cm}^{-2}$  press. The filter is then packed in the form of a 50-mm dia. cylinder, 15 to 20-mm high, according to dust level. It is then weighted again for verification purposes.

The  $\gamma$ -ray spectra of the filters are then measured, on the same detector (HP Ge type N with 50% relative efficiency) six days after the sampling, to get rid of short-lived natural relationship products. The gamma-ray measurement acquisition time is 1000 minutes. The background noise of a blank filter measured and compacted under the same conditions as the sample is deduced systematically. The minimum detectable concentrations (sampled volume about  $70\,000$  to  $100\,000\text{ m}^3$ ), expressed in accordance with reference (CEA, 1989) and the order of magnitude of the usually achieved uncertainties are given in Table 1.

TABLE 1

Minimum detectable concentrations of atmospheric radionuclides for weekly samplings (ASS500 P:  $100\,000\text{ m}^3$  of sampled air) and the order of magnitude of the usually achieved uncertainties

Radionuclides	Minimum detectable concentrations in $\text{Bq.m}^{-3}$	Measurement uncertainties in % ( $\pm 2\sigma$ )
$^7\text{Be}$	3.0 to $5.0 \cdot 10^{-6}$	5 to 10
$^{22}\text{Na}$	2.5 to $3.5 \cdot 10^{-7}$	30 to 40
$^{40}\text{K}$	3.5 to $8.5 \cdot 10^{-6}$	25 to 35
$^{137}\text{Cs}$	3.0 to $5.0 \cdot 10^{-7}$	20 to 40
$^{210}\text{Pb}$	7.0 to $15 \cdot 10^{-6}$	7 to 15

Fig. 11 shows a gamma-ray spectrum obtained for an atmospheric aerosol sampling corresponding to  $106\,000\text{ m}^3$  of filtered air, and the background spectrum of a blank type G3 filter measured on the same detector. In addition to  $^7\text{Be}$ ,  $^{22}\text{Na}$ ,  $^{210}\text{Pb}$ ,  $^{137}\text{Cs}$ , and  $^{40}\text{K}$  gamma lines, we can see those relating to the daughters of  $^{222}\text{Rn}$  ( $^{214}\text{Bi}$ ,  $^{214}\text{Pb}$ ) and  $^{220}\text{Rn}$  ( $^{212}\text{Bi}$ ,  $^{212}\text{Pb}$ ) as well as the activation lines of the radiation of cosmic origin on the germanium and the detector shielding (copper).

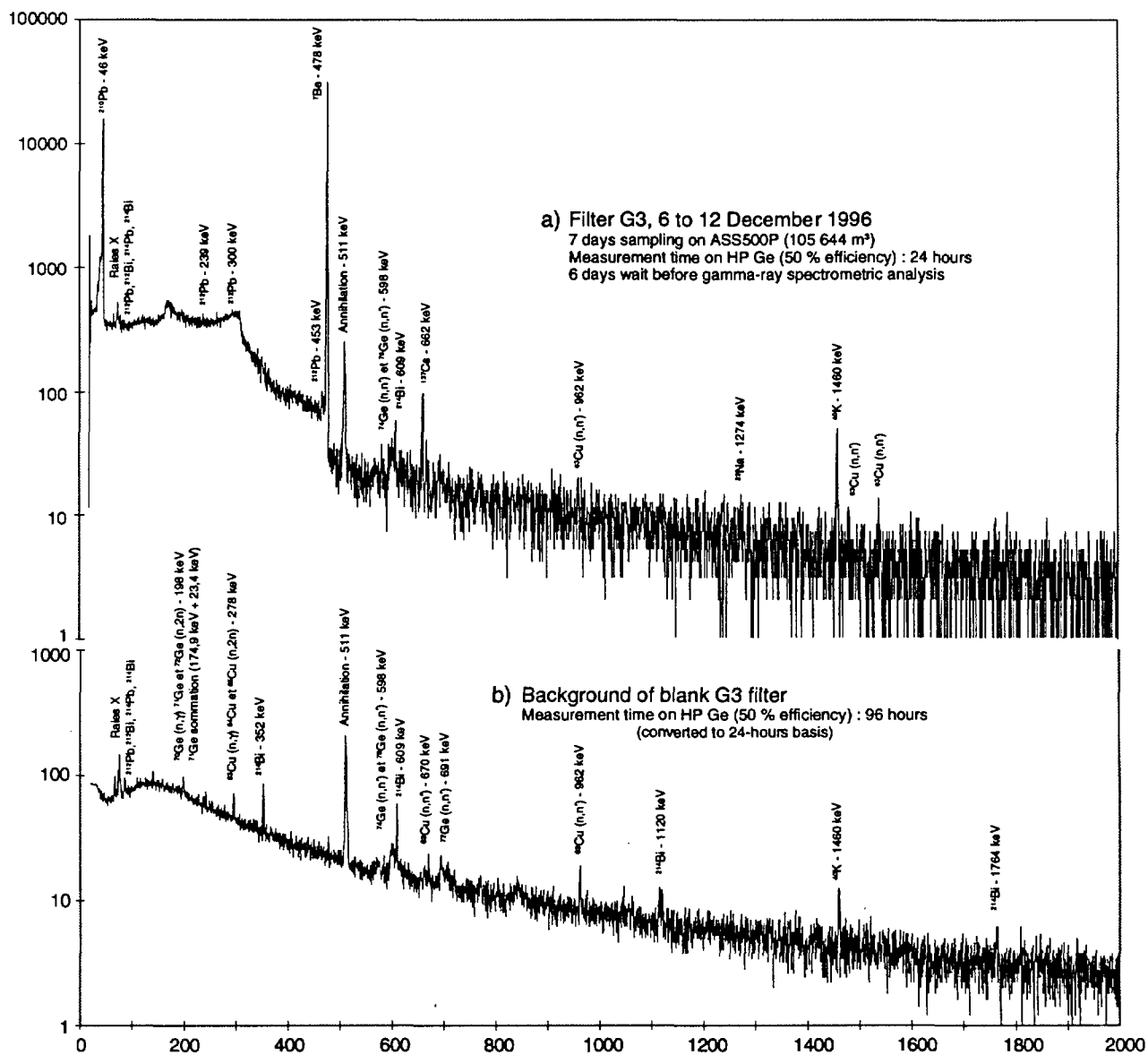
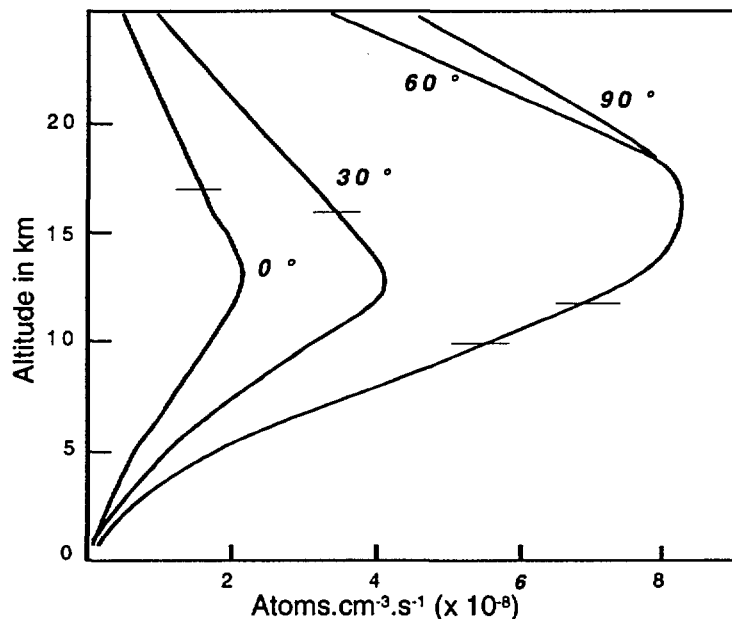


Fig. 11. a) gamma-ray spectrum of a G3 filter (7 days sampling,  $106\,000\text{ m}^3$  of filtered air sampled). b) gamma-ray spectrum of a blank filter

## ATMOSPHERIC RADIOACTIVITY

The main radionuclides detected at Montlhéry, after the decay of the short-lived natural products are  $^7\text{Be}$ ,  $^{22}\text{Na}$ ,  $^{40}\text{K}$ ,  $^{137}\text{Cs}$ ,  $^{210}\text{Pb}$ .  $^7\text{Be}$  is a major radiotracer for understanding the atmospheric transport processes. This is a product of the spallation reactions induced by the high-energy cosmic protons and neutrons on the nitrogen and oxygen atoms of the atmosphere. Beryllium is chemically highly reactive and attaches very rapidly to the atmospheric aerosols after formation. There results that beryllium is essentially attached to particles with submicronic diameters between 0.03 and 1  $\mu\text{m}$  [8]. The production rate of this cosmogenic radionuclide is a function of the altitude and latitude (Fig 12).



**Fig. 12.** Production of  $^7\text{Be}$  under the effect of cosmic radiation, in the atmosphere as a function of altitude and latitude. The horizontal lines indicate the altitude of the tropopause (Jungue, 1973)

The maximum rate is obtained at an altitude of about 12 km (a consequence of the rapid decay of the neutron flux and the variation of the air density with altitude).

$^{22}\text{Na}$  is also a cosmogenic radionuclide formed from nuclear reactions on argon atoms. It is produced in small quantity in the stratosphere. Consequently, it is not systematically detected but generally observed at our latitude in the summer.

The radioactive half-lives of  $^7\text{Be}$  and  $^{22}\text{Na}$ , i.e. 53.3 days and 2.6 years, respectively, are long enough to consider that the concentrations measured in the troposphere come from the stratospheric compartment. Recent models indicate that 49% of the  $^7\text{Be}$  settle on the earth's surface (51% loss by radioactive decay). Table 2 shows the data concerning the production rates of both these radionuclides (Holm, 1994).

TABLE 2  
Production rate and concentration of  $^7\text{Be}$  and  $^{22}\text{Na}$  in the troposphere and the stratosphere

Radio-nuclides	Half-life	Production troposphere (atoms.cm <sup>-2</sup> .s <sup>-1</sup> )	Total production atmosphere (atoms.cm <sup>-2</sup> .s <sup>-1</sup> )	Concentration stratosphere (Bq.kg <sup>-1</sup> air)	Concentration troposphere (Bq.kg <sup>-1</sup> air)
$^7\text{Be}$	53.3 d	$2.7 \cdot 10^{-2}$	$8.6 \cdot 10^{-5}$	0.3	$1 \cdot 10^{-6}$
$^{22}\text{Na}$	2.60 y	$2.4 \cdot 10^{-5}$	$8.1 \cdot 10^{-2}$	0.09	$1 \cdot 10^{-2}$

$^{222}\text{Rn}$ , the parent nucleus of  $^{210}\text{Pb}$ , is released continuously by continental land surfaces and seas, owing to its basic property of being a rare gas, hence virtually free of chemical or physical bonds. The mean release rate of total radon in atmosphere is  $0.72 \text{ atoms.cm}^{-2}.\text{s}^{-1}$  (Roth *et al.*, 1985). By disintegration, the radon gives birth to two successive series of daughters, the last of which leads to the formation of isotopic radioactive  $^{210}\text{Pb}$  with a radioactive half-life of 22 years. The existence of physical and chemical bonds between metal atoms and the atmospheric aerosols has the following effects:

- generally, these daughters of radon are prevented from being injected directly into the atmosphere,
- rapid attachment of the radon daughters produced in air on present aerosols is promoted.

It is generally admitted that about 80% of the  $^{210}\text{Pb}$  is attached to aerosols with a diameter less than or equal to  $1 \mu\text{m}$ , therefore with a negligible gravitational velocity. The behavior of this radionuclide is therefore limited to that of the finest aerosols.

$^{40}\text{K}$  (radioactive half-life  $1.26 \cdot 10^9$  years, relative abundance 0.0118% in natural potassium) is a radionuclide of terrestrial origin. The earth's crust concentration can vary by several orders of magnitude with a mean activity of about  $200 \text{ Bq.kg}^{-1}$ . Further, the mean  $^{40}\text{K}$  contents of ocean waters, about  $12000 \text{ Bq.m}^{-3}$ , is basically at the origin of the presence of this radionuclide in the atmosphere, following exchanges at the ocean-atmosphere interfaces.

$^{137}\text{Cs}$  (radioactive half-life 30.15 years) is an anthropogenic radionuclide and was introduced in the atmosphere mainly as a result of atmospheric nuclear tests conducted in the late fifties and in the sixties (the last (*Chinese*) atmospheric test dates back to 1980) and because of the 1986 Chernobyl accident. In a previous paper (Bourlat *et al.*, 1994), we showed, from our Montlhéry facility, that 40 % of the atmospheric  $^{137}\text{Cs}$  present in measurements carried out from 1991 of ground-level air near Paris can be attributed to atmospheric nuclear tests.

#### ATMOSPHERIC POLLUTION (Jungue, 1973)

The AIRPARIF agency, in charge of monitoring the air quality in the Paris area, uses three types of stations for measuring the main atmospheric pollutants, covering a 100-km radius around Paris:

*Urban background stations:* these are installed away from the direct influence of any industrial or traffic pollution source. They are located in places such as parks, school yards, etc. The primary pollutant (CO, NO, SO<sub>2</sub>) concentration levels are rather low there. The AIRPARIF network comprises 60 stations of this type.

*Rural background stations:* these are installed at the periphery of metropolitan Paris. Their purpose is to measure the impact of certain pollutants created by chemical reactions from primary pollutants. This is the case in particular of O<sub>3</sub>. The network comprises 3 stations of this type.

*Proximity stations:* these are installed at close proximity of motor traffic. They measure NO, CO. The network comprises 9 stations of this type.

The main atmospheric pollutants measured by the AIRPARIF network are CO, NO, NO<sub>2</sub>, O<sub>3</sub> and SO<sub>2</sub>.

Sulphur dioxide SO<sub>2</sub>: sulphide pollution in the atmosphere and in particular that related to SO<sub>2</sub> has been the subject of many papers since it became apparent that its distribution could only be interpreted on a continental and global scale. Sulphides are present in the atmosphere in three major forms: SO<sub>2</sub>, H<sub>2</sub>S and in the sulphide form in aerosols. Knowing the relative abundance and the relationships between these various types is essential to establish a realistic balance of sulphides in the atmosphere.

Several sources of atmospheric SO<sub>2</sub> have been identified:

- production of H<sub>2</sub>S by certain oceans and land, by sulphide reduction. This reduction is the consequence of excessive decomposition of organic matter, resulting in depletion of free oxygen in water (in lakes and in coastal areas), swamps or land. The hydrogen sulphide H<sub>2</sub>S thus released in the atmosphere leads to high production of SO<sub>2</sub> by oxidation.
- production of SO<sub>2</sub> and H<sub>2</sub>S by the volcanic activity. This source seems to play a minor role in the global balance.
- production of SO<sub>2</sub> of industrial origin: SO<sub>2</sub> is a major indicator of the presence of fixed sources, combustion chambers in the industry, heating activities. Owing to the presence of sulphur in automobile fuels (mainly in diesel fuel) sulphur is also a pollutant released in a stray manner in cities, albeit at low concentration levels. The percentage of SO<sub>2</sub> of industrial origin is estimated at about 10% of the total amount released to the atmosphere.

It should further be noted that the surface of the earth plays a pivotal role in the SO<sub>2</sub> balance at global level. It not only acts as a source of gaseous sulphur compounds, but also as an absorbent (absorption of SO<sub>2</sub> by plant, deposition by precipitation and capture by soils).

The SO<sub>2</sub> concentrations in the first layers of the atmosphere are about 10-20 µg.m<sup>-3</sup> in rural areas. Under unfavorable conditions (winter time, temperature inversion, anticyclonic situation, absence of wind) they may reach concentrations of about 100 µg.m<sup>-3</sup> at ground level around industrial sites and near large cities.

NO and NO<sub>2</sub> nitrocompounds: these are produced naturally, on a global scale, from the ground by reduction of nitrides under the action of micro-organisms. It is considered that concentrations corresponding to a production of natural origin are less than 10 µg.m<sup>-3</sup>. They

are also indicative of human activity, in particular near large urban sites (mainly vehicle exhaust gases and power stations). Concentrations, in particular during the winter periods, can then reach several tens of  $\mu\text{g.m}^{-3}$ . In the summer, any high levels of  $\text{NO}_2$ , much lower than in the winter time, are essentially attributable to photochemical reactions.

CO carbon monoxide: contrary to carbon dioxide  $\text{CO}_2$ , whose main source is of natural origin, and whose biological cycle has been the subject of many papers, carbon monoxide is essentially of anthropogenic origin ; it is mainly produced by rapid and incomplete combustion of fuels. Dissociation of  $\text{CO}_2$  into CO only becomes appreciable at altitudes over 100 km.

In rural areas, CO is not measured by AIRPARIF, as this pollutant exhibits concentration levels close to the measuring equipment sensitivity threshold. In urban areas, concentrations may reach several hundreds of  $\mu\text{g.m}^{-3}$ .

Ozone  $\text{O}_3$  (Toupange, 1988; Doury, 1994): Ozone is chemically formed and destroyed within the atmosphere. Ozone formation processes are complex. Knowing ozone distribution in the atmosphere is of utmost importance to determine the global heat and radiation balance of the mesosphere, in particular in the ultraviolet region. Extensive literature, beyond the scope of this study, deals with this aspect.  $\text{O}_3$  concentrations in the troposphere are about  $50 \mu\text{g.m}^{-3}$ , with often irregular variations which strongly depend on the latitude and seasons. Above an altitude of about 30 km, the concentration decreases regularly generally faster than the air density. At ground level, maximum concentrations (about  $70\text{-}100 \mu\text{g.m}^{-3}$ ) are obtained in the summer, in particular near certain industrial sites, which suggests an anthropogenic origin. In this case,  $\text{O}_3$  is formed by photochemical reactions. Nitrogen oxides and hydrocarbons combined with intense insolation produce  $\text{O}_3$ . In the winter however, in particular when weather conditions are very stable, the primary pollutant levels increase (NO in particular). In this type of situation,  $\text{O}_3$  is chemically destroyed by the NO. The measured  $\text{O}_3$  levels are then close to the minimum detectable concentrations.

## COMPARISON OF POLLUTION AND ATMOSPHERIC RADIOACTIVITY MEASUREMENTS

### $\text{SO}_2$ , dust level, $^{210}\text{Pb}$ , $^{137}\text{Cs}$ , $^{40}\text{K}$ comparison

Fig. 13 shows the evolution of the  $\text{SO}_2$  level, measured in Paris ( $2^\circ 20' \text{ E}$ ,  $48^\circ 52' \text{ N}$ ) during year 1996 and January 1997. The measurements were supplied by AIRPARIF and concerns site 13F75 located 500 meters from Place d'Italie. Daily measurements were adjusted to the week corresponding to the ASS500 P atmospheric sampling. Fig. 14 shows the weight of aerosols (dust level) expressed in  $\mu\text{g.m}^{-3}$  of sampled filtered air, collected on each weekly filter. The knowledge of that data is important for human health as atmosphere pollution influences cardio-pulmonary disease, mainly after ingestion of less than  $10 \mu\text{m}$  in size particule. In the vicinity of large urban zones total aerosols concentration in suspension are sometimes larger than indicative values fixed by Health World Organisation. This organisation considers that the mean annual concentration should not exceed  $60$  to  $90 \mu\text{g.m}^{-3}$ . It should be noted that values measured in Montlhéry are closed to the maximum limits fixed

by OMS. Fig. 15, 16 and 17 respectively show the evolution of the specific activities of  $^{210}\text{Pb}$ ,  $^{137}\text{Cs}$ ,  $^{40}\text{K}$ .

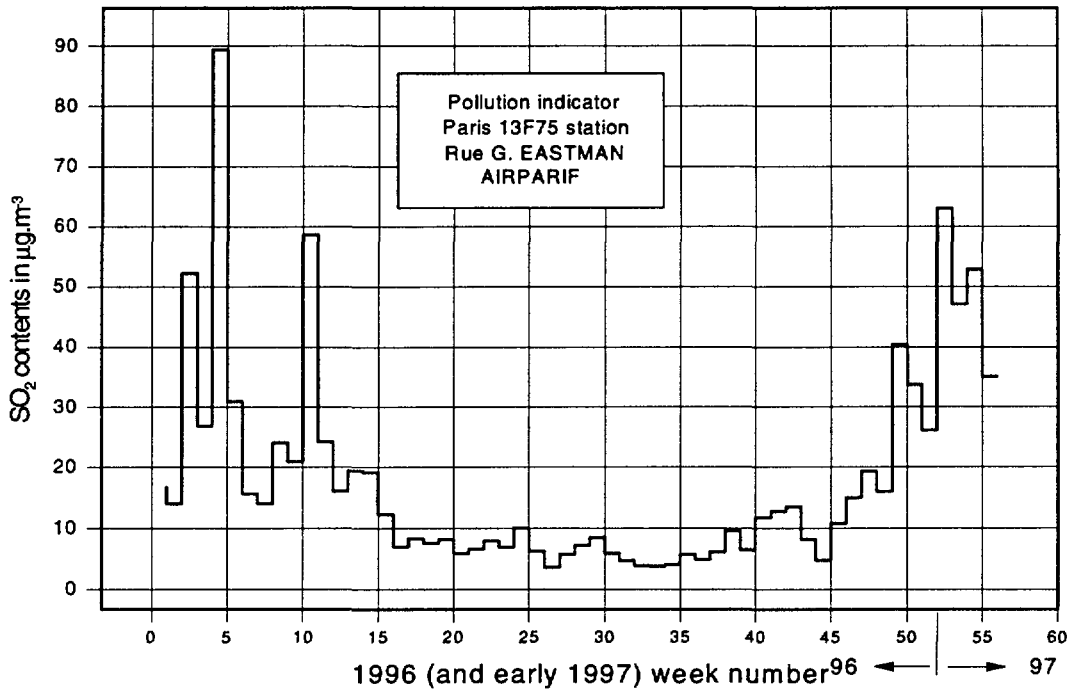


Fig. 13. Evolution of the SO<sub>2</sub> level, measured in Paris (readings were adjusted to the ASS500 P sampling weeks)

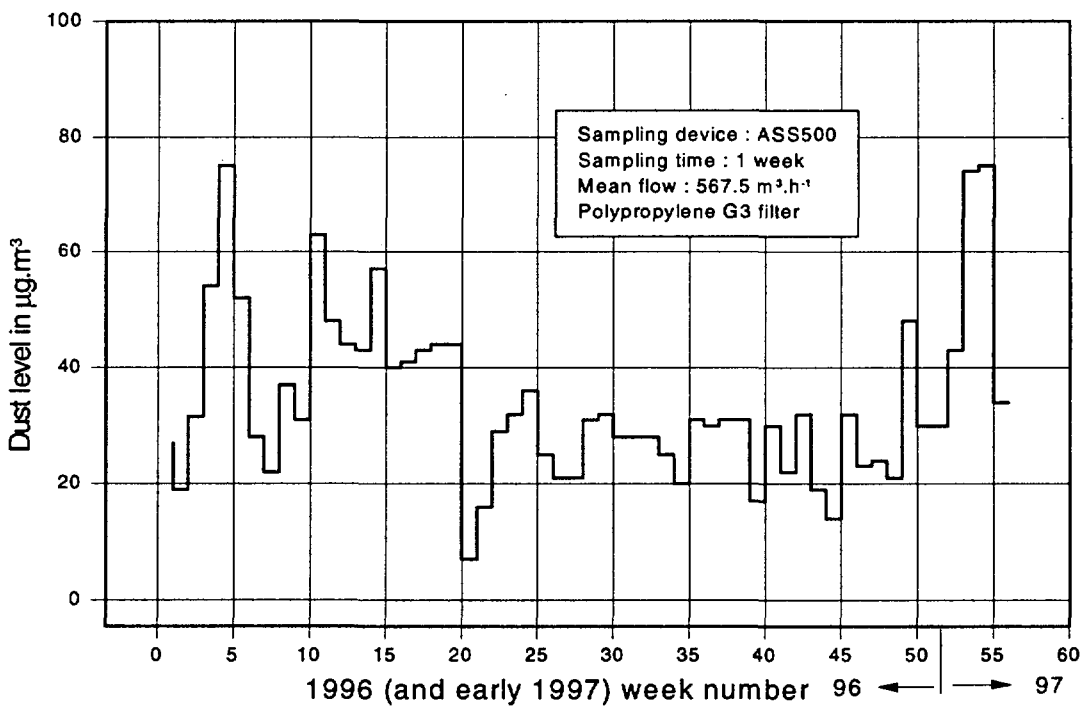


Fig. 14. Evolution of dust level (ASS500 P : 1 sampling week)

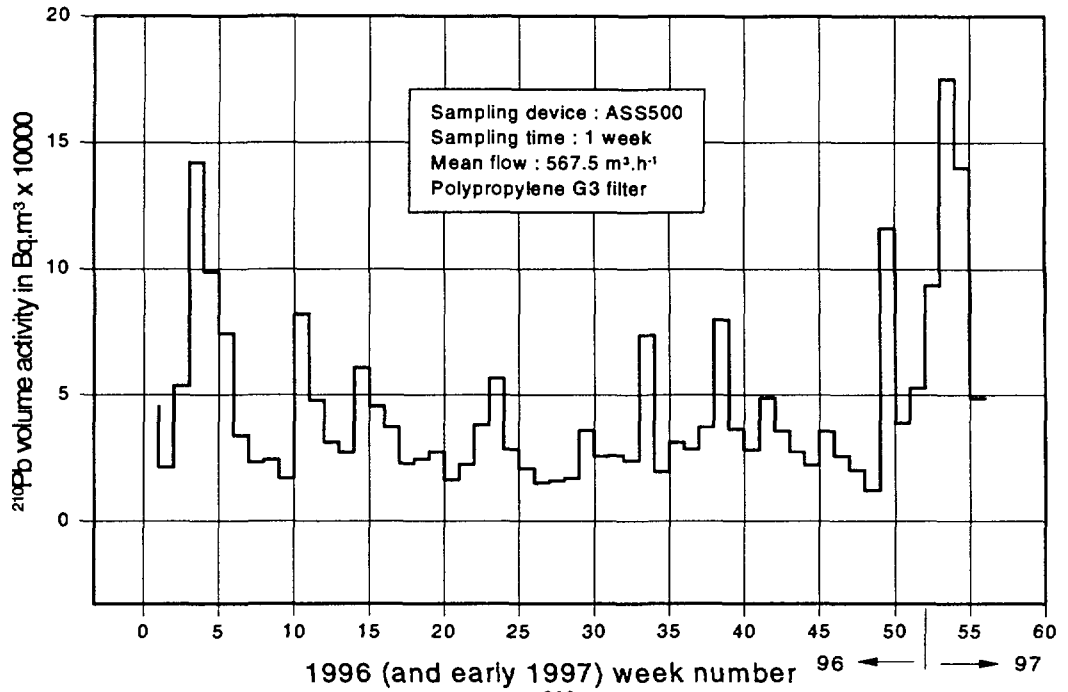


Fig. 15. The activity concentration of  $^{210}\text{Pb}$  (ASS500 P : 1 sampling week)

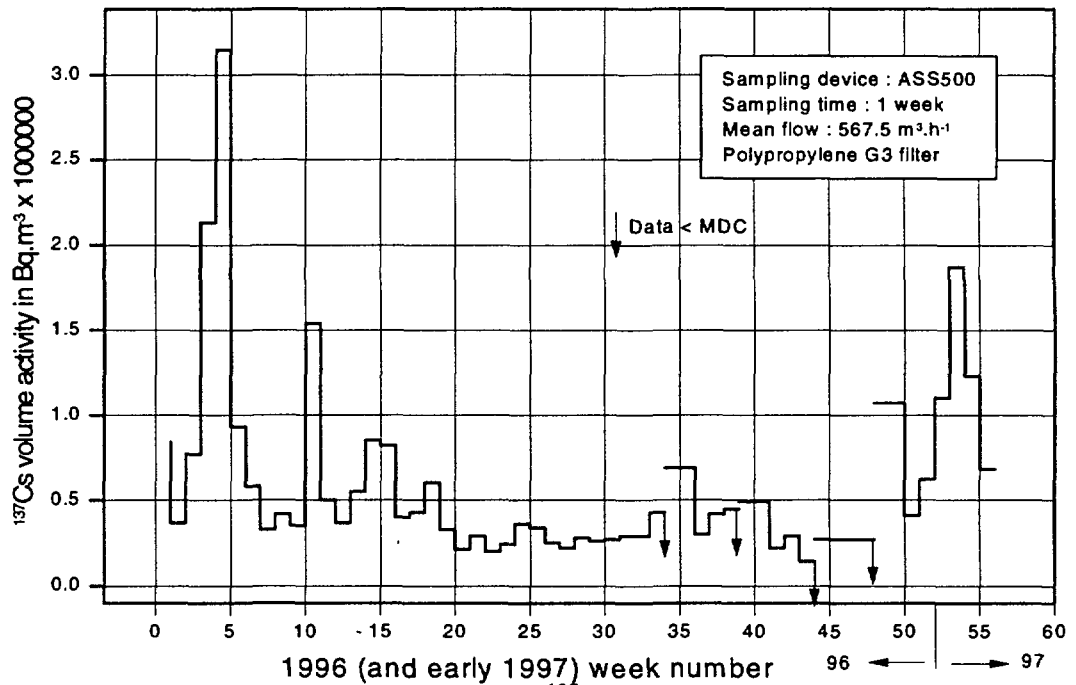


Fig. 16. The activity concentration of  $^{137}\text{Cs}$  (ASS500 P : 1 sampling week)

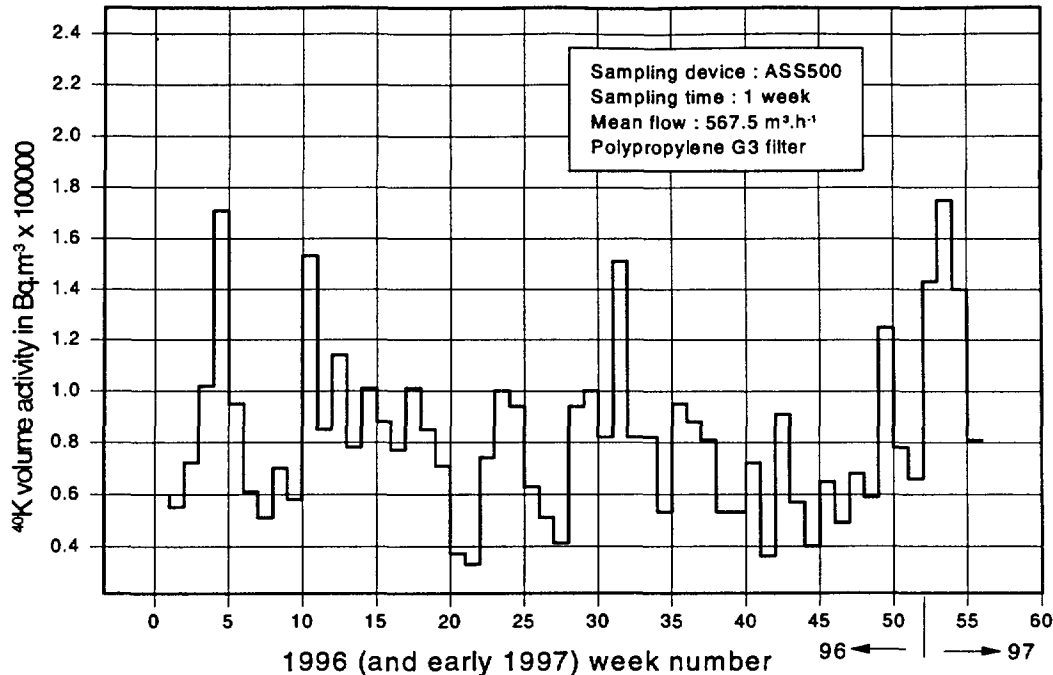


Fig. 17. The activity concentration of  $^{40}\text{K}$  (ASS500 P: 1 sampling week)

We can see a good correlation between the peaks emphasized for  $\text{SO}_2$  with those corresponding to the dust level and the specific activities of  $^{210}\text{Pb}$ ,  $^{137}\text{Cs}$ .

As an exemple, the analysis of the covariance of the observed data for the evolution of  $\text{SO}_2$  and  $^{137}\text{Cs}$  during 1986, lead to a correlation factor ( $r$ ), defined hereafter, of 0.81.

$$r = \frac{\frac{1}{n} \sum (x_i - \mu_x)(y_i - \mu_y)}{\sqrt{\frac{1}{n} \sum (x_i - \mu_x)^2} \times \sqrt{\frac{1}{n} \sum (y_i - \mu_y)^2}}$$

with  $x_i$ ,  $y_i$  observed data ( $\text{SO}_2$  and  $^{137}\text{Cs}$ ) and  $\mu_x$ ,  $\mu_y$  : means of populations  $x_i$  and  $y_i$ .

The specific activities relating to  $^{40}\text{K}$  seem to exhibit a more unique evolution.

Whatever the indicator considered (pollutant, dust level, radionuclides), the main peaks observed correspond to particular periods of time of the year, essentially the winter period (December, January, February) and the March-April period.

The similar evolution of  $^{210}\text{Pb}$  and  $^{137}\text{Cs}$  suggests that the sudden increase in specific activity of these two radionuclides at certain times of year is not due to a local reentrainment of aerosols from the ground. Otherwise, the sensitivity of our sampler and measurements would have emphasized a correlated specific activity in  $^{232}\text{Th}$ . The activity of  $^{228}\text{Ac}$ , a daughter product of  $^{232}\text{Th}$ , is systematically less than the minimum detectable concentration ( $0.5 - 1.5 \times 10^{-6} \text{ Bq.m}^{-3}$ ) during the whole period. Radionuclide  $^{232}\text{Th}$ , of terrestrial origin, can be considered as an excellent tracer of a local reentrainment mechanism in the atmosphere. This

assumption is backed by the study conducted by Hien *et al.* (1993) who measured the  $^{137}\text{Cs}/^{232}\text{Th}$  and  $^{137}\text{Cs}/^{134}\text{Cs}$  ratios at the ground surface and in atmospheric aerosols in 1986 and 1987 at Dalat (Vietnam) after the Chernobyl accident. The authors reached the conclusion of a contribution by a possible dust reentrainment from the ground in the  $^{137}\text{Cs}$  peaks observed at certain times of year.

The peaks relating to  $^{210}\text{Pb}$  and  $^{137}\text{Cs}$  observed in the winter actually denote the atmosphere's climatic changes through the seasons. Considering the size of the aerosols, these changes result in an increase of depositions on ground in the winter, due to precipitation, either through a nucleation mechanism or by impaction (Armengaud *et al.*, 1993). These precipitations are subjected to the effect of the displacements of cold air masses (in particular the continental polar component).

Fig. 18 shows the variations of local meteorological parameters adjusted over the aerosol sampling weeks. Further, some meteorological conjunctions (anticyclonic stability, absence of wind followed by temperature inversion) are at the origin of certain  $\text{SO}_2$  pollution peaks in the Paris area, by blocking pollution dilution in the atmosphere. By analogy, we can consider in this case that the correlated radioactivity peaks essentially correspond to blocking of the atmospheric aerosols near ground.

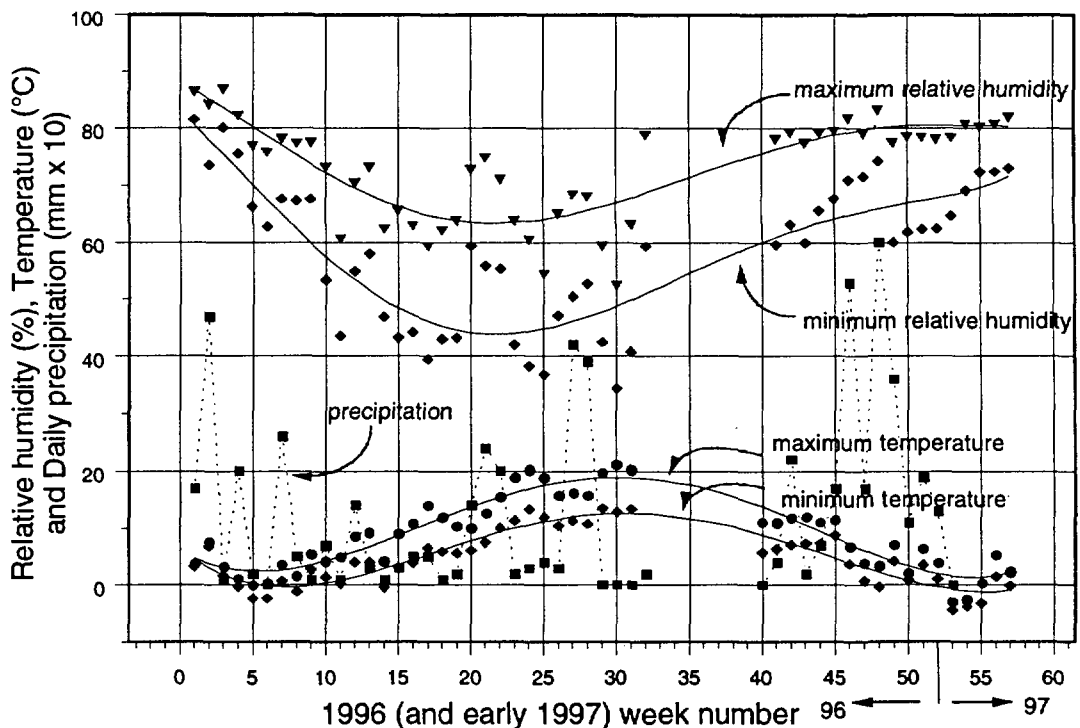


Fig. 18. Evolution of local meteorological parameters (Montlhéry)

This is in particular what was observed, paradoxically, in fair weather periods, both in winter (essentially in January and December 1996) and spring (essentially in March and April), which promote an increase of atmospheric radioactivity (exclusive of nuclear incidents or accidents). This effect is due to the large temperature difference between day and night, which creates in the morning a mass of cold air at ground level, colder than that found at an altitude of a few

hundred meters. This meteorological phenomenon acts as a cover over metropolitan Paris, which does not feature any large natural obstructions.

### $O_3$ , $^7Be$ , $^{22}Na$ comparison

Fig. 19 shows the ozone concentration variation in the air as measured in Paris by AIRPARIF. We can see that the maximum contents are obtained in the dry season, a time when the  $O_3$  production mechanism is intensified (insolation). The same figure shows the evolution of  $^7Be$  during the year. We can again see that maximum values obtained correspond to certain ozone peaks.

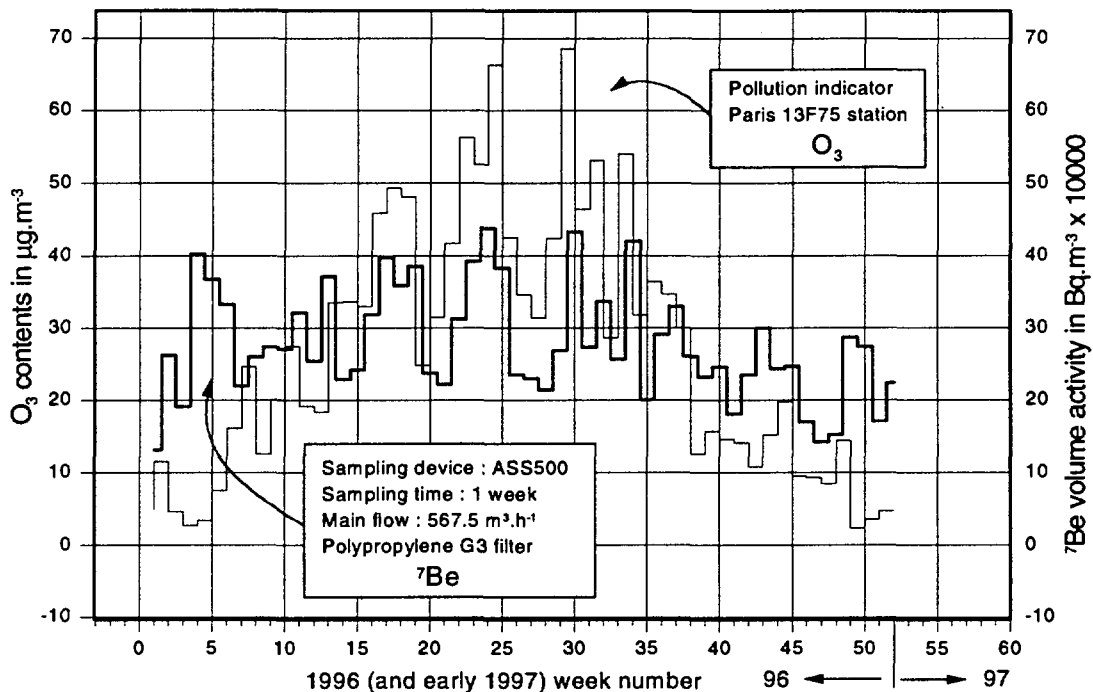


Fig. 19. Compared evolutions of the  $O_3$  contents in Paris and the specific atmospheric activity of the  $^7Be$  (measured at Monthléry using the ASS500 P sampler: 1 sampling week).

$^{22}Na$ , another cosmogenic radionuclide, is also detected mainly in the summer (Fig. 20). According to the Table 1 the uncertainties are large (of order of 50% for the  $^{22}Na$  activities detected). So certain weekly levels are lower than the limit of detection (MDC). The correlation between these two indicators (radionuclides and  $O_3$ ), however, is rather poor and should be considered as a general trend.  $^7Be$ , a cosmogenic product, is formed in the atmosphere by mechanisms which are highly different from those concerning  $O_3$ . A study conducted by Abe *et al.* (1993) shows excellent correlation between the cosmic radiation variation observed at ground level and that observed for  $^7Be$ . This study's conclusion is a poor correlation between the yearly evolution of the  $O_3$  content and the measured  $^7Be$  activity. The peaks observed for the  $^7Be$  (in spring and summer) in insolation periods probably correspond to the transition of these radionuclides from the stratospheric compartment, where they are continuously formed to the tropospheric compartment, and to an increase of the "dry" fine aerosol fallouts. In the other hand the weekly levels of  $^{22}Na$  which are lower than the limit of detection (MDC) seems to be, from Figure 18, correlated with the increase in precipitation.

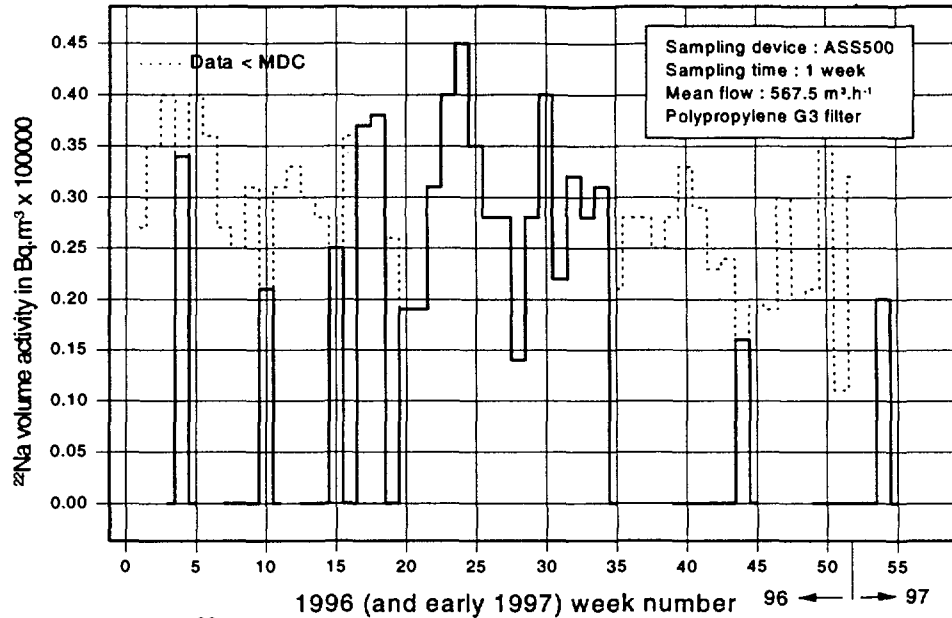


Fig. 20. The  $^{22}\text{Na}$  activity concentration (ASS500 P: 1 sampling week)

### Comparison with the other atmospheric pollutants $\text{NO}_2$ , $\text{NO}$ , $\text{CO}$ .

Fig. 21 shows the yearly evolution of the other pollutants measured in Paris. We observe an evolution close to that observed for  $\text{SO}_2$ , the non-cosmogenic nuclides and dust level. The correlation is particularly good for  $\text{NO}$  and  $\text{CO}$ , which are indicators characteristic of primary pollution (fuel combustion).

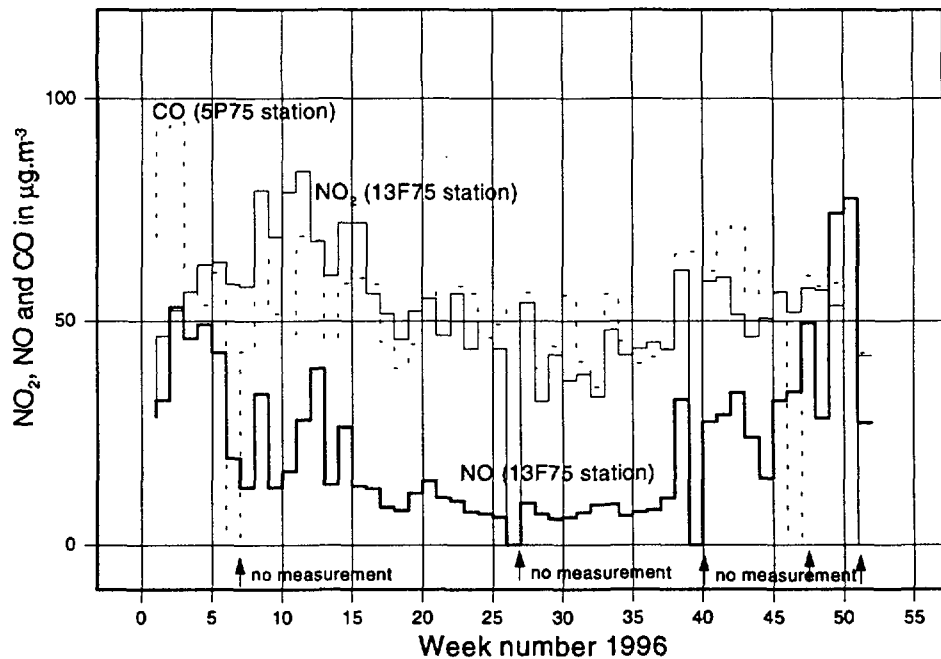


Fig. 21. Compared evolution of pollutants  $\text{CO}$ ,  $\text{NO}$  and  $\text{NO}_2$  measured in Paris (value adjusted on the ASS500P sampling weeks)

The case of NO<sub>2</sub>, which is more complex, has to do with its primary and secondary pollutant nature (photochemical reactions). It should be further noted that stations 5P75 and 13F75 are urban background stations, therefore remote for any direct industrial or automotive pollution sources. The measured concentrations of the various pollutants therefore reflect the mean atmospheric pollution for given meteorological conditions.

## CONCLUSION

Consistent monitoring of the atmospheric radioactivity over a large number of years, both in French Polynesia and the Paris area, using high volume aerosol samplers and low-background HP Ge gamma spectrometry, has emphasized seasonal fluctuations. These fluctuations in atmospheric radioactivity are specific to the measured type of atmospheric radionuclide. Radionuclides of telluric and anthropogenic origin (<sup>210</sup>Pb and <sup>137</sup>Cs) exhibit a maximum evolution in the winter time. The evolution of <sup>40</sup>K in air near Paris is more complex, probably due to the different production sources (from ground but also from seas). We observe a similar trend for SO<sub>2</sub> and NO type pollutants. However, the concentrations of radionuclides of cosmogenic origin (<sup>7</sup>Be, <sup>22</sup>Na) increase in the summer time similar to O<sub>3</sub>, another atmospheric pollutant.

Highlighting correlations between the evolution of radionuclides and certain pollutants present in the atmosphere should promote better understanding of the mechanisms involved on a global scale in the evolution of these atmospheric indicators. To this end, it will be beneficial, in the future, to relate to the measurements of the activity concentration of certain radionuclides to meteorological data (local inversion temperatures, wind rose, displacements of air masses, etc.)

The concurrent use of samplers of very different design and flowrate led us to wonder about the nature of the actually captured particle-size range. Further studies will be necessary to clarify the notion of representativity of the sampling and the systematic uncertainty assigned to the final result, which typically only takes account of the random uncertainty of the measurement.

## ACKNOWLEDGEMENTS

The authors wish to thank Abt D., Girard M. and F. Raynaud F. for their active participation in this study.

## REFERENCES

- Abe M., Kurotaki K., Shibata S. & Takeshita H. (1993). Trend analysis of ten years of changes in radioactive substances in the atmosphere at Chiba, Japan. Proceedings of the international symposium on Isotope techniques in the study of past and current environmental changes in the hydrosphere and atmosphere, Vienna.

- Armengaud A. & Genthon C. (1993). Modelling global distributions of  $^{222}\text{Rn}$ ,  $^{210}\text{Pb}$  and  $^7\text{Be}$  in the atmosphere with general circulation models. Proceedings of the international symposium on Isotope techniques in the study of past and current environmental changes in the hydrosphere and atmosphere, Vienna.
- Arnold D., Jagielak J., Kolb W., Pietruszewski A., Wershofen H. & Zarucki R. (1994). Practical experience in and improvements to aerosol sampling for trace analysis of airborne radionuclides in ground level air. Physikalisch Technische Bundesanstalt report, PTB-Ra-34, Braunschweig.
- Bourlat Y., Milliès-Lacroix J.C. & Abt D. (1994). Measurement of low-level radioactivity in the Modane Underground Laboratory. *N.I.M., A 339*, pp. 309-317
- CEA (Commissariat à l'Énergie Atomique) (1989). Détermination du seuil et de la limite de détection en spectrométrie. Groupe de Travail de Normalisation n°5 du Comité d'Instrumentation de Radioprotection, Rapport CEA-R-5506.
- Davies G. (1973). Air filtration. Academic Press, London New-York.
- Doury A. (1994). Quelques réflexions sur le comportement thermodynamique de l'ozoneosphère. *Pollution Atmosphérique (Janvier-Mars)*. pp. 74-84.
- Hien P.D., Binh N.T., Truong Y., Bac V.T. & Ngo N.T. (1993). Long range transport of caesium isotopes from temperate latitudes to the equatorial zone during the winter monsoon period. Proceedings of the international symposium on Isotope techniques in the study of past and current environmental changes in the hydrosphere and atmosphere, Vienna.
- Holm E. (1994). Radioecology lectures in environmental radioactivity. Lund University Sweden. World Scientific.
- Jungue E. (1973). Air chemistry and Radioactivity. International geophysics series, Academic Press, London, New-York.
- Karol L. (1964). Radioactive isotopes in the atmosphere and their use in meteorology. Conference at Obninsk. Published for the US Atomic Energy Commission and the National Science Foundation, Washington, D.C.
- Milliès-Lacroix J.C., Bourlat Y. & Mosnier R. (1994). Airborne radioactivity measurements in Montlhéry (France), Summary account of measurements made from 1986 through 1992. Proceedings of the International Meeting on Low-Level Air Radioactivity Monitoring, Central Laboratory for Radiological Protection, Madralin (Poland).
- Pruppacher H.R., Semonin R.G. & Slinn W.G.N. (1983). Precipitation scavenging dry deposition and resuspension. Elsevier.
- Roth E. & Poty B. (1985). Méthodes de datation par les phénomènes nucléaires naturels. Collection du Commissariat à l'Énergie Atomique. Masson.
- Sanchez B. & Vendel J. (1995). Mesure de l'efficacité et de la perte de charge de filtres synthétiques. Institut de Protection et de Sécurité Nucléaire, Rapport d'essais Serac/Lecev/95-26.
- Toupange G. (1988). L'ozone dans la basse troposphère. Théorie et Pratique. *Pollution Atmosphérique (Janvier-Mars)*. pp. 32-42.